ISSN 0006-2979, Biochemistry (Moscow), 2011, Vol. 76, No. 10, pp. 1131-1139. © Pleiades Publishing, Ltd., 2011.
Original Russian Text © E. S. Tkacheva, E. V. Leychenko, M. M. Monastyrnaya, M. P. Issaeva, E. A. Zelepuga, S. D. Anastuk, P. S. Dmitrenok, E. P. Kozlovskaya, 2011, published in Biokhimiya, 2011, Vol. 76, No. 10, pp. 1387-1397.
Originally published in Biochemistry (Moscow) On-Line Papers in Press, as Manuscript BM11-147, September 4, 2011.

New Actinoporins from Sea Anemone *Heteractis crispa*: Cloning and Functional Expression

E. S. Tkacheva, E. V. Leychenko, M. M. Monastyrnaya*, M. P. Issaeva, E. A. Zelepuga, S. D. Anastuk, P. S. Dmitrenok, and E. P. Kozlovskaya

Pacific Institute of Bioorganic Chemistry, Far Eastern Branch of the Russian Academy of Sciences, pr. 100 let Vladivostoku 159, 690022 Vladivostok, Russia; fax: (4232) 31-4050; E-mail: rita1950@mail.ru

Received May 13, 2011
Revision received June 7, 2011

Abstract—A new actinoporin Hct-S4 (molecular mass 19,414 ± 10 Da) belonging to the sphingomyelin-inhibited α-pore forming toxin (α-PFT) family was isolated from the tropical sea anemone *Heteractis crispa* (also called *Radianthus macrodactylus*) and purified by methods of protein chemistry. The *N*-terminal nucleotide sequence (encoding 20 amino acid residues) of actinoporin Hct-S4 was determined. Genes encoding 18 new isoforms of *H. crispa* actinoporins were cloned and sequenced. These genes form a multigene Hct-S family characterized by presence of *N*-terminal serine in the mature proteins. Highly conserved residues comprising the aromatic phosphorylcholine-binding site and significant structure–function changes in the *N*-terminal segment (10-27 amino acid residues) of actinoporins were established. Two expressed recombinant actinoporins (rHct-S5 and rHct-S6) were one order less hemolytically active than native actinoporins.

DOI: 10.1134/S0006297911100063

Key words: sea anemone, actinoporin, multigene Hct-S family, recombinant actinoporin, hemolytic activity, structure–function analysis

Actinoporins, the cytolytic protein toxins (20 kDa) produced by venomous sea anemones, are members of the eukaryotic α-pore forming toxin (α-PFT) family [1, 2]. Their activity is determined by the formation of cation-selective pores, 1-2 nm in diameter, in plasmatic membranes containing sphingomyelin [2-5]. The great interest of researchers in actinoporins is due to unique molecular structure allowing their existence both in water-soluble and membrane-associated states and, hence, their use as an apt tool for studying the structural organization and functional mechanisms of natural and artificial membranes [1, 4, 6, 7]. A diversity of biological effects, such as cardioaccelerating, antitumor, and antiparasitic [2, 3], enables constructing (on the basis of the actinoporin structure) advanced highly specific targeted pharmaceutical drugs [8-10].

About 20 α-PFTs from representatives of several sea anemone families have been isolated to date using the methods of structural protein chemistry and molecular biology. Each species contains several actinoporin isoforms: equinatoxins EqtI-IV (*Actinia equina*) [11-13], magnificalysins HMgI-III (*Heteractis magnifica*) [14, 15], sticholysins StnI, II (*Stichodactyla helianthus*) [16, 17], actinoporins RTX-A and RTX-SII (*Radianthus macrodactylus*, syn. *Heteractis crispa*) [18, 19], actinoporins Or-A and Or-G (*Oulactis orientalis*) [20], actinoporins SrcI (*Sagartia rosea*) and PsTX (*Phyllodiscus semoni*) [21, 22]. Recently nucleotide sequences encoding 52 *H. magnifica* magnificalysin isoforms were determined [23]. Each of the actinoporins produced by one sea anemone species is encoded by its own gene, thus belonging to one multigene family [23, 24].

At present the most studied actinoporins are equinatoxin II and sticholysin II, whose 3D structures were determined by X-ray structural analysis and electron microscopy [25, 26], enabling interpretation of many experimental data obtained from the studies on mechanisms of membrane lysing effect [2, 4-7, 27-32] and functional activity of actinoporins [4-6, 8-10, 33].

Earlier four *H. crispa* actinoporins inhibited by sphingomyelin (RTX-A, S, -SII, -G) were isolated and characterized [18, 19, 34]. They possess high hemolytic activity comparable with that of equinatoxin II [11, 12], sticholysin

Abbreviations: a.a., amino acid residue; BLM, bilayer lipid membrane; GST, glutathione S-transferase; IPTG, isopropyl-β-D-1-thiogalactoside; PFT, pore forming toxin.

* To whom correspondence should be addressed.

II [17], and the magnificalysins [14, 15]. The *Radianthus* actinoporins form cation-selective pores, ~1 nm in diameter, in sphingomyelin-containing bilayer lipid membranes (BLMs) and liposomes [7, 27, 35]. Data on the effects of *Radianthus* actinoporins on biological membranes (mammalian erythrocytes and sea-urchin *Strongylocentrotus intermedius* eggs, which membranes do not contain sphingomyelin [27], as well as tumor cell cultures [36]) are indicative of interactions between actinoporins (with implication of RGD-motif) and integrins [37].

The goal of the present study was isolation of the native *H. crispa* actinoporin, cloning of actinoporin Hct-S family genes, production of recombinant proteins, and structure–function analysis of members of this family.

MATERIALS AND METHODS

Chemicals were purchased from Reanal (Hungary), Whatman (UK), ICN Biochemicals (USA), Sigma (USA), SibEnzyme (Russia), Fermentas (Lithuania), Serva (Germany), Merck (Germany), Cryochrome (Russia), and Helicon (Russia).

Biological material. Sea anemones *H. crispa* were collected from the South China Sea littoral in 1990, during the marine expedition on board the "Academician Oparin" research ship. The specimens were stored at –20°C before use. Species identification was performed by E. E. Kostina, Ph. D. (Institute of Marine Biology, Far East Branch of the Russian Academy of Sciences, Vladivostok). Preparation of water extract and sedimentation of protein fraction with acetone was carried out by the previously described method [34]. All procedures were performed at 4°C.

Isolation and purification of proteins. Gel filtration and desalting were carried out on columns, 3 × 100 cm and 2.5 × 30 cm, filled with Acrylex P-4 and equilibrated with 0.01 M ammonium-acetate buffer, pH 6.0, at a flow rate of 18 ml/h (4°C). The fraction volume was 5 ml.

Ion-exchange chromatography on CM-32 cellulose was carried out on a column (2.2 × 45 cm) equilibrated with the same buffer, using a linear 0-0.5 M NaCl gradient, total volume 2 liters. The flow rate was 0.5 ml/min, and fraction volume was 5 ml.

Reverse-phase HPLC of proteins was carried out on a ZORBAX Eclipse® XDB-C_8 column (4.6 × 150 mm) (Agilent, USA), using an Agilent 1100 chromatograph with UV detector (λ = 214 nm), using a stepwise 10-60% acetonitrile gradient in 0.1% TFA, pH 2.2, for 40 min at a flow rate of 0.5 ml/min.

Protein was determined by the Lowry method [38] using bovine serum albumin as standard.

Molecular mass of actinoporin was determined on an ULTRAFLEX III TOF/TOF mass-spectrometer (Bruker Daltonics, Germany). The time-of-flight spectra were recorded both in linear and reflectron modes.

Amino acid sequence of the actinoporin *N*-terminal fragment was determined on a Procise 492 cLC automated solid-phase protein sequencer (Applied Biosystems, USA) using the manufacturer's program.

Cloning of actinoporin genes. cDNA was synthesized using total mRNA isolated from *H. crispa* tentacles [18]. Nucleotide sequences encoding the mature actinoporin were amplified with the following gene-specific primers: 5′-TCGGCGGCTTTAGCTGGCACAATTACTCTC-3′ (forward) and 5′-TTAGCGTGAGATCTTAATTTGCAGTAT-3′ (reverse), constructed using Vector NTI 8 software (Invitrogen, USA) on the basis of known genes encoding *H. crispa* RTX-SII and RTX-S3 proteins [19, 39]. The primers were synthesized by Eurogen (Russia). PCR was carried out on a GeneAmp PCR System 2700 (Applied Biosystems) according to the following protocol: 5 min at 94°C followed by 28 cycles: 30 sec at 94°C (denaturation), 45 sec at 59°C (annealing), 45 sec at 72°C (elongation); and final elongation at 72°C for 15 min. PCR product (550 bp) was isolated from agarose gel using the DNA Extraction Kit (Fermentas) and cloned in pTZ57R/T using the T/A cloning system (Fermentas).

Determination and analysis of nucleotide sequences. Plasmid DNA was isolated from cells by the method of alkaline lysis [40]. Recombinant plasmids were sequenced on an ABI3130 DNA analyzer (Applied Biosystems). Nucleotide and amino acid sequences were analyzed using the Vector NTI 8 program package (Invitrogen).

Expression. For creating expression constructs, the DNA fragment encoding actinoporin was amplified using Vent-DNA-polymerase (SibEnzyme) and gene specific primers 5′-GTCGGCGGCTTTAGCTGGCACAATTACTCTC-3′ (forward, SF) and 5′-CCCCAAGCTTAGCGTGAGATCTTAATTTGCAGTAT-3′ (reverse, SR). For the retention of the endopeptidase site and correct insertion of the gene into the pET-41a(+) vector (Novagen, USA), the nucleotide G was linked to the 5′-end of the forward primer, and the *Hind*III restriction site combined with a stop-codon was inserted into the reverse primer. The PCR product was digested with *Hind*III endonuclease and cloned into the pET-41a(+) vector at the *PshA*I and *Hind*III restriction sites. Thus prepared recombinant plasmids were sequenced and used for transformation of *Escherichia coli* Rosetta (DE3) cells by means of electroporation on a Multiporator device (Eppendorf, Germany) according to the standard protocol [41]. The transformed cells were cultured overnight in 2× YT medium [42] containing kanamycin (50 μg/ml) and chloramphenicol (34 μg/ml) followed by culturing in 100 ml up to A_{600} = 0.5-0.6. Then IPTG (Fermentas; final concentration 0.1 mM) was added for induction of expression, and the cells were additionally grown for 3 h at 30°C for the synthesis of soluble hybrid protein. Then the cells were centrifuged at 8000*g* and washed with PBS [43].

Isolation of recombinant actinoporins. The cells containing the hybrid protein were suspended in five volumes

of PBS and ultrasonicated on a Sonopuls HD 2070 (Bandelin Electronic, Germany) for cell wall disruption. Following centrifugation (10,000*g*), the cell lysate was applied onto Ni^{2+}-CAM-agarose and incubated for 10 min at 4°C under continuous mixing for sorption of the hybrid protein. Protein impurities were removed by washing of the Ni^{2+}-CAM-agarose with 50 mM NaH_2PO_4, pH 8.0, containing 300 mM NaCl and 10 mM imidazole, and then with enteropeptidase buffer (20 mM Tris-HCl, pH 8.0, 50 mM NaCl, and 2 mM $CaCl_2$). Enterokinase (New England Biolabs, UK; 1 U per 20 μg hybrid protein) was added, followed by incubation overnight at room temperature under continuous mixing. Then the Ni^{2+}-CAM-agarose was centrifuged at 3000*g*, and the supernatant was incubated with STI-agarose for elimination of enterokinase.

Proteins in crude extract and recombinant proteins were analyzed by Laemmli's SDS-PAGE [44] in 15% polyacrylamide gel.

Hemolytic activity of actinoporins was determined as described in [34].

Mean hydrophobicity (<H>), mean hydrophobic moment (<μ>), and amino acid charges of the *N*-terminal helical fragment of actinoporins were calculated using HELIQUEST software (http://heliquest.ipmc.cnrs.fr), following the standard hydrophobicity scale of individual residues [45] for an 18-a.a. fragment (residues 10 through 27).

Constructing a theoretical model for actinoporin 3D structure. A model of the spatial structure of Hct-S5 was generated by the homological modeling method with the aid of the SPDBV program [46] and the SWISS-MODEL server [47]. The secondary structure elements were determined using the MolMol program [48]. The *S. helianthus* StnII (PDB code 1gwyA) [26] 3D structure was used as a prototype for constructing the model. The model was optimized in the MOE program [49].

RESULTS AND DISCUSSION

Isolation and purification. Several protocols for isolation of native actinoporins from *H. crispa* have been proposed to date, one of them being based on sedimentation of hemolytically active proteins from aqueous extract with 80% acetone. Gel filtration of total protein on Acrylex P-4 has yielded three fractions (Fig. 1a, peaks *1-3*) possessing hemolytic activity. Earlier, individual actinoporins RTX-A, RTX-S, and RTX-SII were isolated from fractions 1 and 2 [19, 34]. In this study, protein fraction 3 (Fig. 1a) was used for further separation of hemolytically active proteins by cation-exchange chromatography on CM-32 cellulose. As a result, five hemolytically active fractions were obtained (Fig. 1b, peaks *1-5*).

Protein fraction 1 (Fig. 1b) was collected, desalted on a column with Acrylex P-4, and used for further separation by reverse-phase HPLC on a ZORBAX Eclipse® XDB-C_8 column. The HPLC yielded fractions containing proteins with molecular masses (by the data of MALDI mass-spectrometry) from 4 to 6 kDa (peaks *1-5*) and 19.3-19.5 kDa (peaks *6-8*) (Fig. 1c). All fractions were tested for toxicity. Peptides comprising fractions 1 and 2 (molecular masses 4-5 kDa) demonstrated severe neurotoxicity against mice, and fractions 3-5 (molecular masses about 6 kDa) had trypsin-inhibiting activity, thus being of the class of protease inhibitors. As shown earlier [34], both groups of biologically active peptides are found in aqueous extracts of *H. crispa*.

Rechromatography of the hemolytically active protein fraction (Fig. 1c, peak *7*) yielded a homogeneous protein named Hct-S4 (Fig. 1d); its molecular mass determined by MALDI-TOF is 19,414 ± 10 Da.

Amino acid sequence of the *N*-terminal fragment. To identify the protein isolated by HPLC (Fig. 1d), we determined its *N*-terminal amino acid sequence (20 a.a.): SAALAGTIIEGASLGFQILD-, which is identical to the same sequence of actinoporin RTX-S3 deduced from the previously determined nucleotide sequence of the corresponding gene [39]. The difference in molecular masses of these proteins (calculated molecular mass of the recombinant actinoporin rRTX-S3 is 19,390.84 Da) suggests that Hct-S4 obtained in this study is a new member of the *H. crispa* actinoporin family, named Hct-S and characterized by the presence of an *N*-terminal serine residue.

Cloning of actinoporin genes. To determine nucleotide sequences of genes encoding mature actinoporins belonging to the Hct-S family, we constructed primers based on the previously determined nucleotide sequences of the genes encoding *H. crispa* actinoporins RTX-SII and RTX-S3 [19, 39]. The PCR product was a DNA fragment about 550 bp in length. This fragment was cloned in the vector pTZ57R/T. More than 50 clones were tested, and 19 nucleotide sequences were identified with identity of 94 to 99%. Based on these data, we deduced the amino acid sequences of 18 new actinoporins of the Hct-S family (Fig. 2). The sequences of Hct-S5 and Hct-S6 are most representative. We also found that the Hct-S10 sequence is encoded by two genes differing in one synonymous nucleotide substitution. Homology of new actinoporins, RTX-A and RTX-SII [18, 19] prepared earlier, and the recombinant RTX-S3 [39] is 89 to 99%. These data suggest that a whole series of actinoporin isoforms likely belonging to several multigene families is synthesized in *H. crispa*, as they are in *A. equina* [11-13] and *H. magnifica* [23] tentacle tissue. These isoforms were conditionally divided into two groups (Fig. 2) depending on the presence of equivalent amino acid substitutions (E10A, DT78/79NR, H98N, L112F, I121V, A131G, M136L, and K159R) in the RTX-SII and Hct-S family actinoporins. Most of the substitutions are in the *N*-terminal fragment.

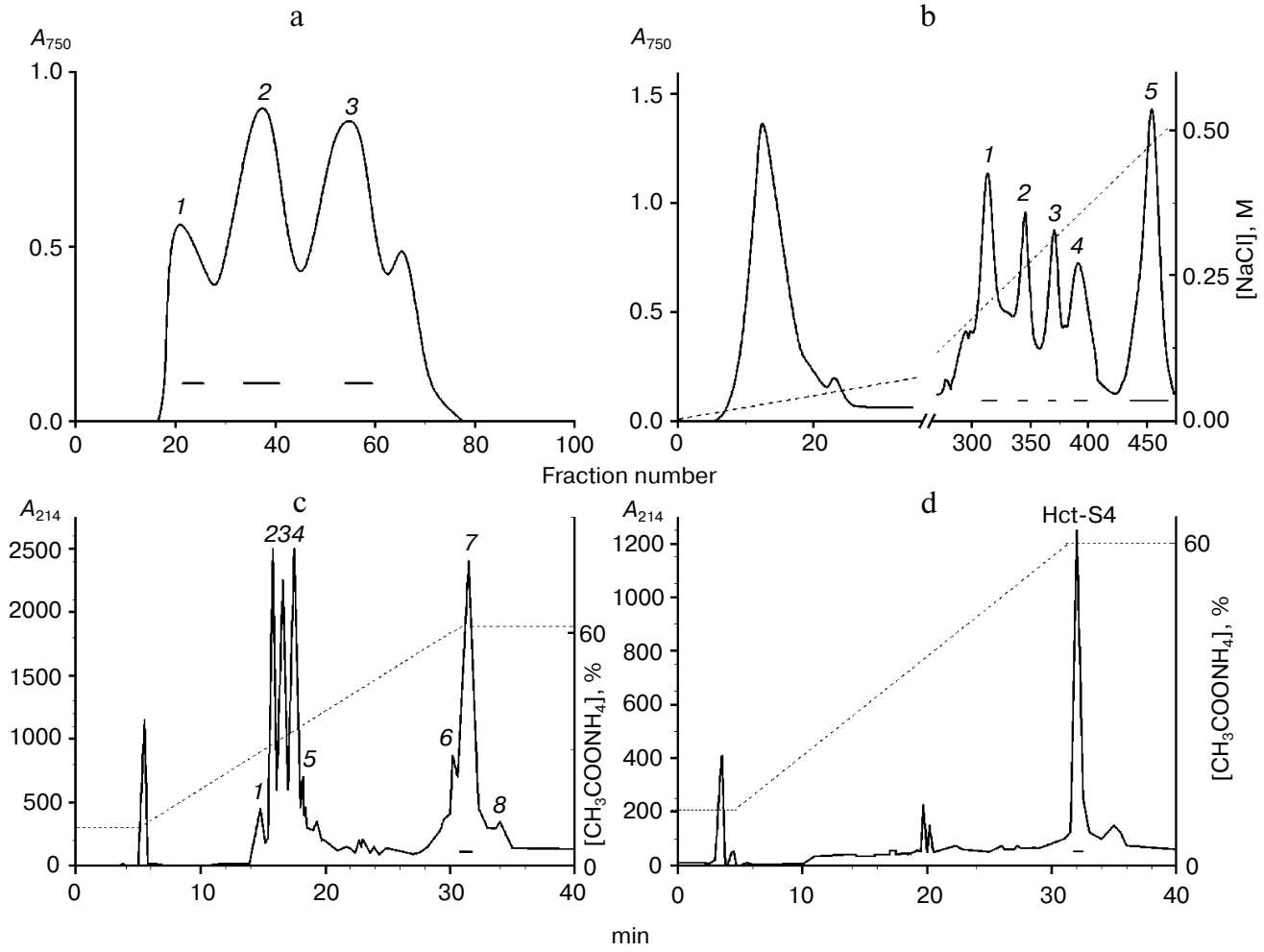

Fig. 1. a) Gel filtration of *H. crispa* proteins on a column (3 × 100 cm) with Acrylex P-4. The fractions possessing hemolytic activity are underlined. b) Cation-exchange chromatography of protein peak *3* (Fig. 1a) on CM-32 cellulose. The confines of hemolytically active fractions are underlined. c) HPLC of fraction 1 after cation-exchange chromatography. d) Rechromatography of fraction 7 (Fig. 1c) under the same conditions.

Expression, isolation, and hemolytic activity of recombinant actinoporins. The most representative sequences Hct-S5 and Hct-S6 were chosen for preparation of expression constructs based on the vector pET41a(+). The recombinant actinoporins rHct-S5 and rHct-S6 were expressed in *E. coli* strain Rosetta (DE3) in the form of hybrid proteins containing the GST-protein, polyhistidine site, and mature actinoporin separated with the enterokinase restriction site. According to the data of electrophoretic analysis, molecular masses of the hybrid proteins were just more than 50 kDa (Fig. 3a), which corresponds to the calculated data (~52 kDa). The recombinant proteins were isolated from cell extract under native conditions by affinity chromatography on Ni^{2+}-CAM-agarose (Fig. 3b). Total yield of recombinant proteins averaged 4 mg per liter of cell culture. The recombinant actinoporins possessed similar molecular masses and isoelectric points and comparable hemolytic activity (Table 1). The hemolytic activity of these proteins was one order of magnitude lower than that of natural actinoporins such as EqtII from *A. equina* [11], StnII from *S. helianthus* [50], HMgI and HMgII from *H. magnifica* [51], RTX-A [34] and RTX-SII [19], as well as recombinant rRTX-S3 from *H. crispa* [39].

Physicochemical properties. Calculated molecular masses of the Hct-S family actinoporins are 19.3-19.5 kDa, which corresponds to molecular masses of natural actinoporins [11, 12, 14, 15, 17, 21, 22, 34]. All members of the family are highly basic polypeptides. Their calculated p*I* values range within 9.10-9.74, which is characteristic of the *Radianthus* actinoporins RTX-A, RTX-S, and RTX-SII, as well as most known actinoporins from other sea anemone species.

Until recently a hallmark of the amino acid composition of actinoporins was believed to be the absence of cysteine residues [1, 2]. However, in 2008 Wang and colleagues found that amino acid sequences of some *H. mag-*

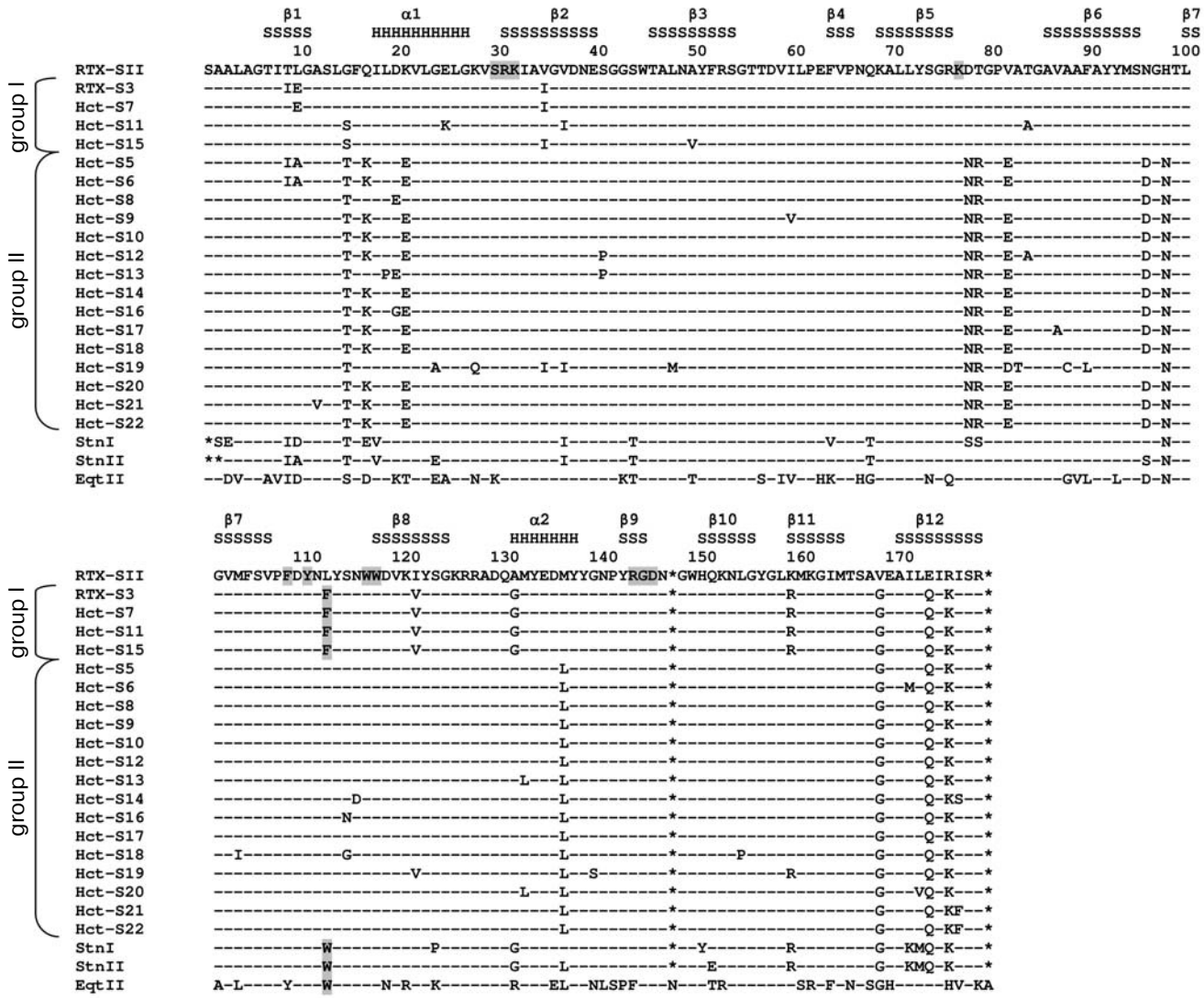

Fig. 2. Multiple alignment of actinoporin amino acid sequences. EqtII, equinatoxin from *A. equina* (SwissProt, P61914); StnI and StnII, sticholysins from *S. helianthus* (SwissProt, P81662, P07845). Amino acids or sequence fragments that are the most essential for pore forming are drawn on a gray background. The letters H and S indicate the length of α-helices and β-strands, respectively.

nifica actinoporins deduced from 52 nucleotide sequences [23] contain this residue at one or more positions, e.g. 15, 36, 110, 133, and 165. Figure 2 shows that most deduced sequences of the Hct-S family actinoporins do not contain cysteine residues, except for the Hct-S19, which contains only Cys88.

Structure–function analysis of Hct-S family actinoporins. In accordance with the data of biochemical, biophysical, X-ray structural, and electron microscopic studies of EqtII and StnII [25, 26], the fist stage of interaction between actinoporin monomer and membrane is formation of tight hydrophobic contacts, as well as hydrogen and ionic bonds, between the aromatic amino acids of the POC-binding site (sequence 108-**F**DYNL**Y**SN**W**W-117 and residues **Y**133, **Y**137, **Y**138) and the phosphorylcholine head groups of membrane sphingomyelin and phosphatidylcholine [26]. Then conformational changes occur involving the highly charged loop 30SRK32, which like a hinge turns out the *N*-terminal fragment to the lipid–water interface of the membrane. This process is accompanied by elongation of the *N*-terminal α-helix and is terminated by its inclusion into the membrane [26]. A functional pore is formed by the *N*-terminal fragments of four actinoporin molecules, which together with membrane phospholipids form a toroidal pore according to the data of Kristan et al. [31]. Since the members of the Hct-S family and EqtII and StnII share 64 through 99% amino acid sequence identity, we suppose that the former have similar mechanism of membranotropic activity.

The 3D structural model of Hct-S5 (Fig. 4) was constructed for structure–function analysis of family members. The 3D structure of StnII (PDB code 1gwyA) from

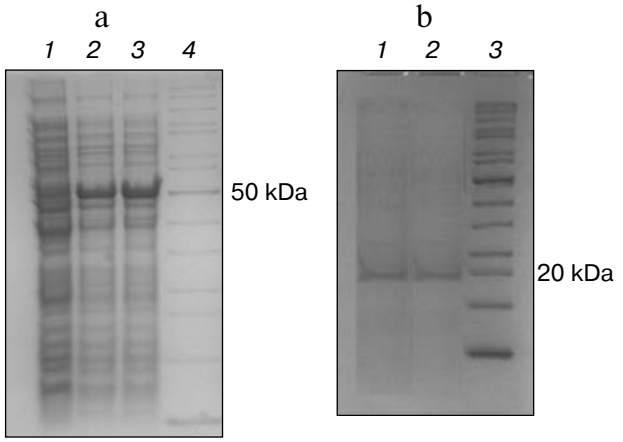

Fig. 3. a) SDS-PAGE of cell lysates after expression: *1*) control (expression of pET41a(+)/hct-s5 without IPTG); *2*) pET41a(+)/HCT-S5; *3*) pET41a(+)/HCT-S6; *4*) molecular mass markers. b) SDS-PAGE of recombinant actinoporins: *1*) rHct-S5; *2*) rHct-S6; *3*) molecular mass markers.

sea anemone *S. helianthus*, which like *H. crispa* belongs to the family Stichodactylidae, was used as prototype. In accordance with the theoretical 3D model, actinoporin Hct-S5 is composed of 12 β-strands and two framing α-helices localized at the *N*- and *C*-ends. The antiparallel β-strands are connected with each other and with α-helical fragments with loops of different length. Figure 4 shows positions and lengths of the two α-helices and 12 β-strands in the Hct-S family actinoporin amino acid sequences.

Most globular proteins with amphiphilic helical fragments 18 a.a. and more in length on their *N*-termini are known to exhibit membranotropic activity [52]. The values of the mean hydrophobic moment <μH> of these fragments usually range within 0.3-0.4, which is indicative of their high capability of being incorporated into the hydrophobic lipid core of membranes. We estimated the hydrophobicity of the recombinant RTX-S3, Hct-S5, and Hct-S6 *N*-terminal fragments by calculating their <H> and <μH> values. Given the amphiphilic nature of the actinoporin *N*-terminal fragments and theoretical data of Eisenberg et al. [53], we used a fragment from 10 to 27 a.a. for calculation of these values, because it is known that residues 17-25 of the fragment of the molecule in aqueous solution are helical [26], and elongation of the α-helix occurs during the interaction of residues 10-16, 26, and 27 with the membrane interface [30]. In accordance with the calculated <H> and <μH> values, these fragments of actinoporins RTX-S3, Hct-S5, and Hct-S6 lie within the range required for strong hydrophobic interactions with fatty acid residues of lipids (Table 2).

Positively charged amino acid residues organized in a network [54, 55] providing interaction between protein molecules and negatively charged phosphorylcholine groups of membrane lipids are equally important for binding of amphiphilic protein structures with a membrane. This pattern holds for α-PFT in sea anemones [30]. In agreement with Schiffer–Edmundson helical rings [56] (not shown), the negatively charged amino acid residues prevail over the positively charged ones on the polar surface of the *N*-terminal helical sites of actinoporins. The presence of the highly basic loop 30SRK32 and positively charged K21 (in RTX-SII and RTX-S3) or K17 (in Hct-S5 and Hct-S6) lysine residues determine electrostatic interaction of these polypeptides with the water–membrane interface. The presence of several negatively charged amino acid residues inside the formed pore lumen determining the actinoporin hemolytic activity is one of necessary conditions for the functional activity of actinoporins. The structures of *N*-terminal fragments in Hct-S family recombinant proteins correspond to the necessary requirements for high pore-forming activity because they possess negatively charged amino acids at the following positions: E10, D20, E25 (in rRTX-S3) and D20, E21, E25 (in rHct-S5 and rHct-S6). Lower hemolytic activity of recombinant rHct-S5 and rHct-S6 proteins compared with rRTX-S3 protein (Table 2) can

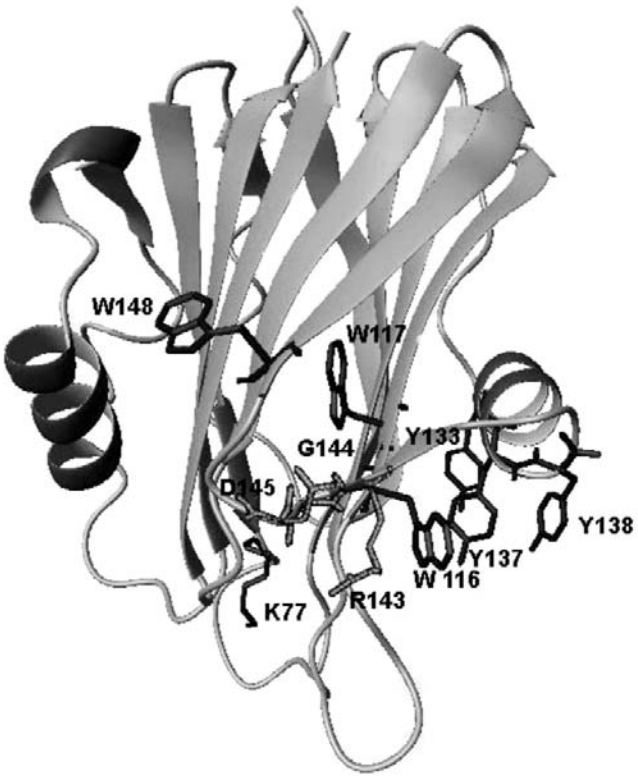

Fig. 4. Ribbon model of the Hct-S5 3D-structure. Secondary structure elements: *N*- and *C*-terminal α-helices are drawn in black and β-strands in gray. Highly conserved Trp and Tyr comprising the POC-binding site (black) and the RGD-motif (gray) are shown as conventional molecular models.

Table 1. Physicochemical properties and hemolytic activities of recombinant actinoporins belonging to the Hct-S family and natural actinoporins RTX-A [34], RTX-SII [19], EqtII [11], StnII [17], HMgI and HMgII [50]

Actinoporin	Molecular mass, kDa	p*I*	Hemolytic activity, HU/mg protein
rRTX-S3	19.39*	9.31**	33 000***
rHct-S5	19.33*	9.33**	1000***
rHct-S6	19.39*	9.10**	1000***
RTX-A	20.0	9.8	35 000
RTX-SII	19.28	10.0	36 000
EqtII	19.0	10.5	36 000
StnII	17.6	9.8	31 000
HMgI	19.0	9.4	36 000
HMgII	19.0	10.0	33 000

* Calculated from amino acid sequence.
** Calculated using the PROPKA 3.0 program [51].
*** Mean values from three independent experiments.

be attributed to the positively charged K17 residue, partially blocking the pore permeability for K^+.

The functional importance of the K77 residue localized in the loop between the β5 and β6 strands and participating in EqtII oligomerization [57] has been demonstrated earlier by cysteine scanning mutagenesis. The hemolytic activity of EqtII-C77 is almost 100 times lower than that of equinatoxin II. Figure 2 demonstrates the presence of a lysine residue within the sequences of all Hct-S family proteins as well as of native actinoporins. The amino acid residues at positions 78-79, which are localized in this loop, are of interest as well. The sequence analysis of Hct-S, the group I actinoporins, demonstrated the presence of GluThr79 dipeptide, which distinguishes them from the members of group II containing AsnArg79 at these positions. rHct-S5 and rHct-S6 (members of group II) containing AsnArg79 dipeptide are found to have lower hemolytic activity than rRTX-S3 (group I).

The majority of amino acid residues forming the membrane-binding POC site [26] are highly conserved, which is typical of members of the actinoporin family. Residues Trp112 and Trp116 localized at the major loop joining the β7 and β8 strands and exposed outside were demonstrated earlier as the key residues in the equinatoxin II aromatic cluster, because their point mutations decrease its ability to bind lipid matrix and decrease EqtII hemolytic activity by more than 90% [29]. Penton has recently shown [10] that the StnI molecule with Trp111 residue (which is analogous to EqtII-Trp112) substituted for Cys demonstrates 8-fold decreased activity in the mutant as compared with the native protein. However, these facts contradict similar data for hemolytic activities of RTX-A, RTX-S, and RTX-SII, the native *Radianthus* actinoporins, PsTX-20A, the native *Phyllodiscus* actinoporin [21], and HMgII and III magnificalysins [14], containing Leu or Phe residues at the position equivalent to EqtII-Trp112. Recently, Bakrac et al. showed that Tyr113, a residue present in all known actinoporins and in all sequences of Hct-S family, is necessary, in addition to Trp112, for binding membrane sphingomyelin [58]. We suppose that Trp112 residue, if present or not in an actinoporin molecule, does not play a principal role in its hemolytic activity because other aromatic residues (Tyr113, 133, 137, 138, and Trp116) endow the molecule the ability to form strong contacts with a phosphorylcholine group of membrane sphingomyelin (hydrogen bonds, hydrophobic and π-cation interactions), which is supported by experimental [7] and unpublished calculated data.

Table 2. Mean hydrophobicity (<H>) and mean hydrophobic moment (<μH>) of the *N*-terminal α-helical actinoporin fragments

Actinoporin	<μH>	<H>	Number of charged amino acid residues in the fragment 10-27	
			(−) charge	(+) charge
RTX-A	0.349	0.563	2	1
RTX-SII	0.278	0.609	2	1
rRTX-S3	0.402	0.479	3	1
rHct-S5	0.392	0.523	3	1
rHct-S6	0.392	0.523	3	1

Obviously, the controversy in the experimental data can be explained by the existence of other functionally important regions of the molecule, such as the ArgGlyGlu145 tripeptide, also participating in membranotropic action of actinoporin (data not published) and localized at the actinoporin surface near the POC site.

Apparently, the hemolytic activity is influenced not only by the substitution of residues at any distinct position of the molecule, but mostly by the presence and localization of positively and negatively charged residues in the functionally significant N-terminal fragment of the actinoporin.

In spite of significant successes in the study of structural and functional relationships of α-PFT in sea anemones, details of their membrane binding processes, association, inclusion into lipid bilayer, and pore formation are not yet clear. The mutant forms of *Heteractis* actinoporins with amino acid substitutions at the functionally significant POC site, *N*-terminal fragment, and RGD motif will be studied further for better understanding of the pore formation mechanism.

The authors are indebted to Drs. O. V. Chernikov and K. V. Guzev from the Pacific Institute of Bioorganic Chemistry of the Far East Branch of the Russian Academy of Sciences for the *N*-terminal sequencing of actinoporin and nucleotide sequencing.

This work was supported by the Program of Russian Academy of Sciences Presidium "Molecular and Cellular Biology" (Grant No. 09-I-P22-05), Far East Branch of the Russian Academy of Sciences Grants Nos. 09-III-A-05-141 and 11-III-B-05-009, and the Russian Foundation for Basic Research grant No. 10-08-00316-a.

REFERENCES

1. Parker, M. W., and Feil, S. C. (2005) *Prog. Biophys. Mol. Biol.*, **88**, 91-142.
2. Anderluh, G., and Macek, P. (2002) *Toxicon*, **40**, 111-124.
3. Turk, T. J. (1991) *Toxicol.-Toxin. Rev.*, **10**, 223-262.
4. Brezhestovsky, P. D., Monastyrnaya, M. M., Kozlovskaya, E. P., and Elyakov, G. (1988) *Dokl. Akad. Nauk SSSR*, **299**, 748-750.
5. Belmonte, G., Pederzolli, C., Macek, P., and Menestrina, G. (1993) *J. Membr. Biol.*, **131**, 11-22.
6. Shnyrov, V. L., Monastyrnaya, M. M., Zhadan, G. G., Kuznetsova, S. M., and Kozlovskaya, E. P. (1992) *Biochem. Int.*, **26**, 219-229.
7. Chanturia, A. N., Shatursky, O. Ya., Lishko, V. K., Monastyrnaya, M. M., and Kozlovskaya, E. P. (1990) *Biol. Membr. (Moscow)*, **7**, 763-769.
8. Potrich, C., Anderluh, G., Macek, P., and Menestrina, G. (2000) *Acta Biol. Sloven.*, **43**, 47-51.
9. Tejuca, M., Anderluh, G., and Dalla Serra, M. (2009) *Toxicon*, **54**, 1206-1214.
10. Penton, D., Perez-Barzaga, V., Diaz, I., Reytor, M. L., Campos, J., Fando, R., Calvo, L., Cilli, E. M., Morera, V., Castellanos-Serra, L. R., Pazos, F., Lanio, M. E., Alvarez, C., Pons, T., and Tejuca, M. (2011) *PEDS*, **24**, 485-493.
11. Macek, P., and Lebez, D. (1981) *Toxicon*, **19**, 233-240.
12. Anderluh, G., Pungercar, J., Strukelj, B., Macek, P., and Gubensek, F. (1996) *Biochem. Biophys. Res. Commun.*, **220**, 437-442.
13. Belmonte, G., Menestrina, G., Pederzolli, C., Krizaj, I., Gubensek, F., Turk, T., and Macek, P. (1994) *Biochim. Biophys. Acta*, **1192**, 197-204.
14. Wang, Y., Chua, K. L., and Khoo, H. E. (2000) *Biochim. Biophys. Acta*, **1478**, 8-18.
15. Samejima, Y., Yanagisaws, M., Aoki-Tomomutsu, Y., Iwasaki, E., Ando, J., and Mebs, D. (2000) *Toxicon*, **38**, 259-264.
16. Blumenthal, K. M., and Kem, W. R. (1983) *J. Biol. Chem.*, **258**, 5574-5581.
17. Lanio, M. E., Morera, V., Alvarez, C., Tejuca, M., Gomez, T., Pazos, F., Besada, V., Martinez, D., Huerta, V., Padron, G., and Chavez, M. (2001) *Toxicon*, **39**, 187-194.
18. Il'ina, A., Lipkin, A., Barsova, E., Issaeva, M., Leychenko, E., Guzev, K., Monastyrnaya, M., Lukyanov, S., and Kozlovskaya, E. (2006) *Toxicon*, **47**, 517-520.
19. Klyshko, E. V., Issaeva, M. P., Monastyrnaya, M. M., Il'ina, A. P., Guzev, K. V., Vakorina, T. I., Dmitrenok, P. S., Zykova, T. A., and Kozlovskaya, E. P. (2004) *Toxicon*, **44**, 315-324.
20. Il'ina, A. P., Monastyrnaya, M. M., Isaeva, M. P., Guzev, K. V., Rasskazov, V. A., and Kozlovskaya, E. P. (2005) *Rus. J. Bioorg. Chem.*, **31**, 320-324.
21. Nagai, H., Oshiro, N., Takuwa-Kuroda, K., Iwanaga, S., Nozaki, M., and Nakajima, T. A. (2002) *Biosci. Biotechnol. Biochem.*, **66**, 2621-2625.
22. Jiang, X. Y., Yang, W. L., Chen, H. P., Tu, H. B., Wu, W. Y., Wei, J. W., Wang, J., Liu, W. H., and Xu, A. L. (2002) *Toxicon*, **40**, 1563-1569.
23. Wang, Y., Yap, L. L., Chua, K. L., and Khoo, H. E. (2008) *Toxicon*, **51**, 1374-1382.
24. Anderluh, G., Krizaj, I., Strukelj, B., Gubensek, F., Macek, P., and Pungercar, J. (1999) *Toxicon*, **37**, 1391-1401.
25. Athanasiadis, A., Anderluh, G., Macek, P., and Turk, D. (2001) *Structure*, **9**, 341-346.
26. Mancheno, J. M., Martin-Benito, J., Martinez-Ripol, M., Gavilanes, J. G., and Hermoso, J. A. (2003) *Structure*, **11**, 1-20.
27. Kozlovskaya, E. P., Ivanov, A. S., Mol'nar, A. A., Grigor'ev, P. A., Monastyrnaya, M. M., Khalilov, E. M., and Elyakov, G. B. (1984) *Dokl. Akad. Nauk SSSR*, **277**, 1491-1493.
28. Alvarez, C., Casallanovo, F., Shida, C. S., Nogueira, L. V., Martinez, D., Tejuca, M., Pazos, F. I., Lanio, M. E., Menestrina, G., Lissi, E., and Schreier, S. (2003) *Chem. Phys. Lipids*, **122**, 97-105.
29. Hong, Q., Gutierrez-Aguirre, I., Barlic, A., Malovrh, P., Kristan, K., Podlesek, Z., Macek, P., Turk, D., Gonzalez-Manas, J. M., Lakey, J. H., and Anderluh, G. (2002) *J. Biol. Chem.*, **277**, 41916-41924.
30. Malovrh, P., Viero, G., Dalla Serra, M., Podlesek, Z., Lakey, J. H., Macek, P., Menestrina, G., and Anderluh, G. (2003) *J. Biol. Chem.*, **278**, 22678-22685.
31. Kristan, K., Podlesek, Z., Hojnik, V., Gutierrez-Aguirre, I., Guncar, G., Turk, D., Gonzalez-Manas, J. M., Lakey, J. H., Macek, P., and Anderluh, G. (2004) *J. Biol. Chem.*, **279**, 46509-46517.

32. Alegre-Cebollada, J., Onaderra, M., Gavilanes, J. G., and Martinez del Pozo, A. (2007) *Curr. Prot. Peptide Sci.*, **8**, 558-572.
33. Alvarez, C., Mancheno, J. M., Martinez, D., Tejuca, M., Pazos, F., and Lanio, M. E. (2009) *Toxicon*, **54**, 1135-1147.
34. Monastyrnaya, M. M., Zykova, T. A., Apalikova, O. V., Shwets, T. V., and Kozlovskaya, E. P. (2002) *Toxicon*, **40**, 1197-1217.
35. Rudnev, V. S., Likhatskaya, G. N., Kozlovskaya, E. P., Monastyrnaya, M. M., and Elyakov, G. B. (1984) *Biol. Membr. (Moscow)*, **1**, 1019-1024.
36. Fedorov, S., Dyshlovoy, S., Monastyrnaya, M., Shubina, L., Leychenko, E., Kozlovskaya, E., Jin, J-O., Kwak, J-Y., Bode, A. M., Dong, Z., and Stonik, V. (2010) *Toxicon*, **55**, 811-817.
37. Monastyrnaya, M., Leychenko, E., Issaeva, M., Likhatskaya, G., Zelepuga, E., Kostina, E., Trifonov, E., Nurminski, E., and Kozlovskaya, E. (2010) *Toxicon*, **56**, 1299-1314.
38. Lowry, O. H., Rosebrough, N. J., Farr, A. L., and Randall, R. J. (1951) *J. Biol. Chem.*, **193**, 265-275.
39. Tkacheva, E. S. (2010) *Vestnik FEB RAS (Moscow)*, **4**, 134-137.
40. Sambrook, J., and Russel, D. W. (2001) in *Molecular Cloning. Laboratory Manual*, 3rd Edn., Cold Spring Harbor Laboratory Press, New York, pp. 1.31-1.58.
41. Sambrook, J., and Russel, D. W. (2001) in *Molecular Cloning. Laboratory Manual*, 3rd Edn., Cold Spring Harbor Laboratory Press, New York., pp. 1.119-1.122, 15.14-15.19.
42. Sambrook, J., and Russel, D. W. (2001) in *Molecular Cloning. Laboratory Manual*, 3rd Edn., Cold Spring Harbor Laboratory Press, New York., p. A2.4.
43. Sambrook, J., and Russel, D. W. (2001) in *Molecular Cloning. Laboratory Manual*, 3rd Edn., Cold Spring Harbor Laboratory Press, New York., p. A1.7.
44. Laemmli, U. K. (1970) *Nature*, **227**, 680-685.
45. Fauchere, J., and Pliska, V. (1983) *Eur. J. Med. Chem.*, **8**, 369-375.
46. http://expasy.org/spdbv
47. Schwede, T., Kopp, J., Guex, N., and Peitsch, M. (2003) *Nucleic Acids Res.*, **31**, 3381-3385.
48. Koradi, R., Billeter, M., and Wuthrich, K. (1996) *J. Mol. Graph.*, **14**, 51-55.
49. http://www.chemcomp.com/Corporate Information/MOE.html
50. Khoo, K. S., Kam, W. K., Khoo, H. E., Gopalakrishnakone, P., and Chung, M. C. M. (1993) *Toxicon*, **31**, 1567-1579.
51. Olsson, M. H. M, Sondergard, C. R., Rostkowski, M., and Jensen, J. H. (2011) *J. Chem. Theory Comput.*, **7**, 525-537.
52. Saier, M. H., Jr., and McCaldon, P. (1988) *J. Bacteriol.*, **170**, 2296-2300.
53. Eisenberg, D., Schwarz, E., Komaromy, M., and Wall, R. (1984) *J. Mol. Biol.*, **179**, 125-142.
54. Seelig, J. (2004) *Biochim. Biophys. Acta*, **1666**, 40-50.
55. Lee, K. H., Hong, S. Y., Oh, J. E., Kwon, M., Yoon, J. H., Lee, J., Lee, B. L., and Moon, H. M. (1998) *Biochem. J.*, **334**, 99-105.
56. Schiffer, M., and Edmundson, A. B. (1967) *Biophys. J.*, **7**, 121-135.
57. Anderluh, G., Barlic, A., Potrich, C., Macek, P., and Menestrina, G. (2000) *J. Membr. Biol.*, **173**, 47-55.
58. Bakrac, B., Gutierrez-Aguirre, I., Podlesek, Z., Sonnen, A. F.-P., Gilbert, R. J. C., Macek, P., Lakey, J. H., and Anderluh, G. (2009) *J. Biol. Chem.*, **283**, 18665-18677.